Published in final edited form as:
Bioorg Med Chem Lett. 2013 July 15; 23(14): 4253–4257. doi:10.1016/j.bmcl.2013.04.096.

Design, synthesis and evaluation of inhibitor of apoptosis protein (IAP) antagonists that are highly selective for the BIR2 domain of XIAP

Robert J. Ardecky[a,b,†], **Kate Welsh**[a,†], **Darren Finlay**[a], **Pooi San Lee**[a,b], **Marcos González-López**[a,b], **Santhi Reddy Ganji**[a,b], **Palaniyandi Ravanan**[a], **Peter D. Mace**[a], **Stefan J. Riedl**[a], **Kristiina Vuori**[a,b], **John C. Reed**[a,b], and **Nicholas D. P. Cosford**[a,b,*]

[a]Program in Apoptosis and Cell Death, NCI-Designated Cancer Center, 10901 North Torrey Pines Road, La Jolla, CA 92037, USA

[b]Conrad Prebys Center for Chemical Genomics, Sanford-Burnham Medical Research Institute, 10901 North Torrey Pines Road, La Jolla, CA 92037, USA

Abstract

We recently reported the systematic ligand-based rational design and synthesis of monovalent Smac mimetics that bind preferentially to the BIR2 domain of the anti-apoptotic protein XIAP. Expanded structure-activity relationship (SAR) studies around these peptidomimetics led to compounds with significantly improved selectivity (> 60-fold) for the BIR2 domain vs. the BIR3 domain of XIAP. The potent and highly selective IAP antagonist **8q (ML183)** sensitized TRAIL-resistant prostate cancer cells to apoptotic cell death, highlighting the value of this probe compound as a valuable tool to investigate the biology of XIAP.

Keywords

Apoptosis; XIAP; Monovalent Smac mimetics; Probe compounds

With an estimated 12.1 million new cases of malignant disease diagnosed every year resulting in approximately 7.6 million deaths worldwide, cancer represents a significant public health concern and a substantial burden on society.[1] Despite progress in the last several years towards the development of improved cancer medications, current therapeutic agents remain prone to intrinsic or acquired resistance, which is a major barrier to effective treatment.[2] The evasion of apoptosis (programmed cell death) by tumorigenic cells is one of the defining hallmarks of cancer and is an underlying cause of therapeutic resistance.[3] The development of therapeutic agents that correct defective apoptotic signaling and allow cell death to proceed selectively in malignant cells is therefore an approach with great promise for the treatment of cancer.

*Corresponding author.
†These authors contributed equally to this work.

Supplementary Material

Supplementary Figures are provided showing the effects of compounds on cells (alone or in combination with TRAIL or TNF) and NMR spectra for **8q**.

The inhibitor of apoptosis proteins (IAPs) have attracted attention recently as potential targets for the development of new cancer therapeutics.[4] Distinct members of the IAP family of antiapoptotic proteins inhibit caspases, the group of intracellular cysteine proteases which act as executioner enzymes by performing apoptosis in cells.[5] Thus, inhibition of specific IAPs de-represses caspases, allowing apoptosis to occur in malignant cells but not normal cells. Human X-linked inhibitor of apoptosis protein (XIAP) is the most potent caspase inhibitor in the IAP family.[6] XIAP contains three ~70 amino acid motifs termed baculovirus IAP repeat (BIR) domains (designated 1, 2, and 3), with two of these BIRs exhibiting specificity for different caspases. The BIR2 domain and an adjacent linker peptide between BIR1 and BIR2 of XIAP combine to mediate the two-site interaction with the apoptosis effector proteases caspases-3 and -7, whereas the BIR3 domain of XIAP targets the apoptosis initiator protease caspase-9.[7]

In the intrinsic cell death pathway, apoptotic signaling is regulated by the mitochondrial protein Smac, an endogenous dimeric proapoptotic antagonist of XIAP. The release of Smac from the inter-membrane space of the mitochondria into the cytosol perpetuates the apoptotic signal by competing with caspases for binding to the BIR domains of XIAP.[8] The design of peptidomimetics that bind to the BIR3 domain of XIAP and in part mimic the activity of Smac has been investigated by a number of research groups and companies that have developed antagonists of XIAP.[4,9] For example, the Genentech group recently reported the discovery and characterization of the clinical candidate peptidomimetic GDC-0152 (**1**, Figure 1).[10] While some success has been achieved using this approach, it has become clear that other strategies for alleviating the repression of caspases by XIAP should also be viable therapeutically. Since all apoptotic signaling, triggered via either the intrinsic or the extrinsic pathway, converges on caspases-3 or -7, it would seem logical to develop XIAP inhibitors with high affinity for the BIR2 domain of XIAP. However, somewhat surprisingly there have been few reports on the design and synthesis of compounds that effect inhibition by binding to the BIR2 domain of XIAP.[11]

We recently described the systematic rational design and synthesis of new monovalent IAP antagonists that bind preferentially to the BIR2 domain of XIAP.[12] Using the AVPI motif found at the N-terminus of Smac as an initial template, we developed the tripeptide model shown in Figure 2. We then synthesized a series of analogues and determined their binding affinity for the BIR2 or BIR3 domains of XIAP. In this initial study we held constant the N-methyl alanine moiety at the P1 position and the proline residue at P3, while investigating the effects of varying the P2 position (R^2) and the C-terminal substituent (R^4). This led to the discovery of compounds such as **2a** (R^4 = NHPh) and **2b** (R^4 = 1-naphthyl) with preferential affinity for XIAP BIR2 vs. BIR3 and promising cell killing activity. We also confirmed that a tetrahydronaphthyl C-terminal capping group (R^4) confers selectivity for BIR3 and potent cell killing activity, as observed for peptidomimetic **2c**. Herein we report our further investigation of the SAR around this series of tripeptides leading to the discovery of novel compounds with unique selectivity for the BIR2 domain of XIAP.

The present study is a continuation of work performed within the Molecular Libraries Probe Production Centers Network (MLPCN; http://mli.nih.gov/mli/mlpcn/) with the goal of developing novel XIAP BIR2-selective probes. In this phase of the study we synthesized analogues that retained the P2 substituent (R^2) as valine and the optimized C-terminal capping groups while varying the substituents at P3 (Figure 2). Modifications were also made to the P1 substituents in some of the optimized compounds. The general synthesis of the tripeptide analogues **8** is illustrated in Scheme 1. Condensation of Boc-amino acid derivative **3** with amino acid derivative **4**, followed by acidic cleavage of the N-terminal Boc protecting group afforded dipeptide **5**. Condensation of dipeptide **5** with the Boc-protected derivative **6** followed by hydrogenolysis of the benzyl ester afforded the tripeptide acid **7**.

Finally, condensation of **7** with the appropriate amine followed by removal of the Boc group provided the target IAP inhibitors **8**.[13]

All compounds synthesized were evaluated for their ability to bind the BIR2 or BIR3 domains of XIAP by employing fluorescence-polarization (FP) competition assays.[14] The results are expressed as competitive inhibition constants (K_i), derived from the corresponding IC_{50} values by application of a mathematical equation developed by Wang and coworkers.[15]

We first synthesized and tested a series of analogues where P1 = NMeAla, P2 = Val and R^4 = 1,2,3,4-tetrahydronaphthyl, while varying the P3 residue. The results are shown in Table 1. The specific amino acid residues that were incorporated into the tripeptide scaffold were selected to maximize diversity and to probe the size of the binding pocket in the P3 region of the protein. Thus, several of the amino acids chosen for P3 contained long chain substituents, some of which were hydrophilic and others with hydrophobic characteristics. Compared with the lead structure **2c** (P3 = Pro) none of the new analogues had improved affinity for the BIR3 domain of XIAP. For example, replacing Pro with Ala at P3 as in **8a** led to a reduction in potency of two-fold for BIR2 and fourteen-fold for BIR3 compared with **2c**. However, it is noteworthy that some analogues with long chain residues at P3 (*e.g.* **8b**, **8d**, **8g**) bound with submicromolar affinity to the BIR3 domain, including the $ArgNO_2$ analogue **8b**, with a K_i value of 0.29 μM at XIAP BIR3 and 12:1 selectivity for BIR3 vs. BIR2. Interestingly, the BIR3 affinity for **8b** (0.29 μM) is comparable with the clinical compound **1** (GDC-0152) (0.26 μM). These results suggest that the BIR3 domain of XIAP tolerates relatively bulky substituents in the P3 region.

We next investigated a set of analogues that retained P1 = NMeAla, P2 = Val and introduced phenylhydrazine into the R^4 position. The results of varying the P3 residue among the analogues are shown in Table 2. For compound **2a**, where P3 = Pro, we had previously found that a phenylhydrazine C-terminal capping group (R^4) confers selectivity for BIR2 of XIAP.[12] In the new series this trend proved to hold true regardless of the P3 residue. In fact, the BIR2 vs. BIR3 selectivity ratio of potencies for all the new compounds was equal to or better than the 3 : 1 ratio exhibited by the potent XIAP antagonist **2a**. Furthermore, the BIR3 potency of the compounds was poor, with none of them exhibiting K_i values better than 8 μM. Although the BIR2 K_i value of 0.39 μM for **2a** was not improved upon, the selectivity of several compounds for BIR2 was significantly better. For example, the next most potent compounds in this series were **8j** (BIR2 K_i = 1.18 μM) and **8p** (BIR2 K_i = 1.88 μM) with $ArgNO_2$ and Lys residues at P3, respectively. The selectivity of these compounds was encouraging, with BIR2 : BIR3 ratios of 7.5 and 11.4 to 1, respectively. Of particular note were the data for **8h** (P3 = Ala) and **8i** (P3 = Val) with BIR2 K_i values of 2.29 μM and 3.04 μM, respectively, and an impressive BIR2 : BIR3 selectivity ratio of more than 20 : 1. Taken together, these data suggest that analogues in which P3 = Ala or Val exhibit favorable selectivity for XIAP BIR2 versus BIR3.

The data for our final iteration of analogues are shown in Table 3. In this series we initially synthesized analogues of the potent XIAP antagonist **2b**, in which R^4 = 1-naphthyl, by varying the P3 substituent. As noted above, we previously found that compound **2b** (with P3 = Pro) is a potent inhibitor of XIAP BIR2 but the BIR2 : BIR3 selectivity ratio is only 3.4 : 1. Using the knowledge gained from the series with R^4 = NHPh (Table 2), we prepared analogues with P3 = Ala (**8q**), Val (**8r**) or OrnCBZ (**8s**). Gratifyingly, we found that all three analogues were selective for BIR2, and essentially inactive against BIR3 with K_i values > 39 μM. In particular, compound **8q**[16] exhibited very respectable potency against XIAP BIR2 with K_i = 1.74 μM. Remarkably, the analogue **8t** in which P1 = Ala (R = H) rather than NMeAla is highly potent against BIR2 (K_i = 0.64 μM) and more than sixty-fold selective for

BIR2 over BIR3. Interestingly, the corresponding analogue in the R^4 = N-phenylhydrazine series (**8x**, Table 3) did not quite exhibit the same BIR2 potency enhancement compared with the parent compound (**8h**, Table 2). Analogues of **8t** in which R = CH_2OH (**8u**) or R^1 = Et (**8v**) were also highly selective for BIR2, although less potent. An analogue of **8q** in which R^4 = naphthalen-1-ylmethanamine (**8w**) retained the BIR2 selectivity of the parent compound but also with reduced BIR2 potency (K_i = 3.00 μM). Overall, the combination of P3 = Ala and R^4 = 1-naphthyl provides XIAP antagonists with excellent BIR2 selectivity and good *in vitro* potency. Despite the excellent potency and selectivity of **8t**, unfortunately when tested in a cellular assay **8t** did not show any activity, presumably due to a lack of cell permeability (see Figure S1 in the Supplementary Material). We therefore proceeded with additional characterization of **8q** as the optimal probe for studies in cells.

Based on these encouraging results we then sought to explore whether the selectivity of compound **8q** for the BIR2 domain of XIAP might be explained by the relative structural properties of the BIR2 and BIR3 domains. Thus we modeled the binding of **8q** onto the Smac binding groove of a BIR2 domain. We chose the structure of XIAP BIR2 from our earlier structure of the caspase-3–BIR2 complex.[7] In addition to being the only available crystal structure of a XIAP/cIAP BIR2 domain, this structure also depicts “Smac-like” binding by the N-terminus of the caspase-3 small subunit to XIAP BIR2 (Figure 3a).[7] Using this interaction we overlaid the structure of **8q** into the Smac-binding groove, conserving the backbone geometry of residues 310–312 from the N-terminus of the caspase-3 small subunit. Conformational freedom of the 1-naphthyl ring permitted by the surrounding protein was explored followed by energetic minimization of the compound, and the lowest energy result is displayed in Figure 3b.

This model suggests several factors that could contribute to the BIR2 selectivity of **8q**. Firstly, as already visualized in the contact from the caspase-3 BIR2 structure, a small non-proline entity is highly compatible with P3-binding adjacent to His223 of BIR2 (Figure 3). In the template caspase-3/BIR2 contact structure (Figure 3a) this residue is valine, and recent publications suggest an alanine in this position to be favorable for BIR2 selectivity.[17,18] The alanine moiety of **8q** allows a similar backbone conformation in P3 (Figure 3b). Secondly, the model (Figure 3b) visualizes that the 1-naphthyl ring is positioned between the aliphatic stems of Lys206 and Lys208 with a plausible positive effect on the interaction of **8q** with the BIR2 domain. These residues correspond to glycine and threonine residues respectively in the BIR3 domain of XIAP, thus negating a potentially favorable interaction.

We next determined the activity of the new inhibitors in a disease-relevant cellular assay. In particular, the ability to sensitize TRAIL-resistant cells to apoptosis was investigated. Thus, PPC-1 prostate cancer cells were exposed to each compound (5 μM) for 4 h, followed by the addition of various concentrations of TRAIL, and incubated for 20 h.[19] Cell viability was then assessed using ATP content as a readout (ATPlite). As shown in Figure 4, the cell penetrant IAP antagonists **2a–c** or **8q** all act synergistically with TRAIL to reduce the number of viable cells to much lower levels than those observed with TRAIL alone. The LD_{50} values for TRAIL in the presence of the compounds **2b**, **2c**, or **8q** (5 μM) are in the 0.073–0.089 nM range. Compound **2b** (5 μM) also acts synergistically with various concentrations of TNF to induce cell death in MDA-MB-231 cells (see Figure S2 in the Supplementary Material). To evaluate the effects in normal cells, compounds **2b** and **8q** were tested against human foreskin fibroblasts (HFF) (Figure 5). No toxicity was observed, even in the presence of TRAIL (100 ng/mL). Furthermore, **8q** showed no toxicity against Fa2N-4 immortalized human hepatocytes (LC_{50} > 50μM).[20] Taken together, these data suggest that our new compounds are cell penetrant and exhibit effects on prostate cancer cells consistent with their observed *in vitro* activity as IAP antagonists.

In conclusion, by using a ligand-based rational design approach we have systematically optimized small molecule monovalent IAP antagonists that inhibit XIAP by binding selectively to the BIR2 domain without interacting with the BIR3 domain at detectable levels. The *in vitro* probe compound **8t** binds to the BIR2 domain with submicromolar affinity and > 60-fold selectivity for BIR2 over BIR3. In addition, the XIAP inhibitory potency observed *in vitro* translates into cell killing activity in prostate cancer cells for the cell penetrant probe **8q**. Consistent with our previous observations with IAP antagonists,[21] the highly BIR2 selective, cell penetrant analogue **8q** showed no toxicity as a single agent (Figures 4, 5 and S1) but rather sensitized the cells to TRAIL-induced apoptosis. Our results suggest that these compounds are potentially useful tools for probing apoptosis signaling pathways in cells. Further optimization of these compounds towards the discovery of potent and selective drug-like analogues is currently in progress.

Supplementary Material

Refer to Web version on PubMed Central for supplementary material.

Acknowledgments

This work was supported by NIH grants HG005033 and R01CA163743 to J.C.R., and R01AA017238 to S.J.R The authors thank Andrey Bobkov for expert technical assistance. M.G.L. acknowledges Fundación Ramón Areces for a postdoctoral fellowship.

References and notes

1. http://www.cancerresearchuk.org/cancer-info/cancerstats/world/cancer-worldwide-the-global-picture
2. Gottesman MM. Annu Rev Med. 2002; 53:615. [PubMed: 11818492]
3. Hanahan D, Weinberg RA. Cell. 2000; 100:57. [PubMed: 10647931]
4. (a) Fulda S, Vucic D. Nat Rev Drug Discovery. 2012; 11:109.(b) Condon S. Ann Rep Med Chem. 2011; 46:211.
5. Pop C, Salvesen GS. J Biol Chem. 2009; 284:21777. [PubMed: 19473994]
6. Schimmer AD, Dalili S, Batey RA, Riedl SJ. Cell Death Differ. 2006; 13:179. [PubMed: 16322751]
7. Riedl SJ, Renatus M, Schwarzenbacher R, Zhou Q, Sun C, Fesik SW, Liddington RC, Salvesen GS. Cell. 2001; 104:791. [PubMed: 11257232]
8. Shiozaki EN, Shi Y. Trends Biochem Sci. 2004; 39:486. [PubMed: 15337122]
9. (a) Sun H, Nikolovska-Coleska Z, Yang C-Y, Qian D, Lu J, Qiu S, Bai L, Peng Y, Cai Q, Wang S. Acc Chem Res. 2008; 41:1264. [PubMed: 18937395] (b) Mannhold R, Fulda S, Carosati E. Drug Discov Today. 2010; 15:210. [PubMed: 20096368] (c) Flygare JA, Fairbrother WJ. Expert Opin Ther Pat. 2010; 20:251. [PubMed: 20100005]
10. (a) Flygare JA, Beresini M, Budha N, Chan H, Chan IT, Cheeti S, Cohen F, Deshayes K, Doerner K, Eckhardt SG, Elliott LO, Feng B, Franklin MC, Reisner SF, Gazzard L, Halladay J, Hymowitz SG, La H, LoRusso P, Maurer B, Murray L, Plise E, Quan C, Stephan J-P, Young SG, Tom J, Tsui V, Um J, Varfolomeev E, Vucic D, Wagner AJ, Wallweber HJA, Wang L, Ware J, Wen Z, Wong H, Wong JM, Wong M, Wong S, Yu R, Zobel K, Fairbrother WJ. J Med Chem. 2012; 55:4101. [PubMed: 22413863] (b) Erickson RI, Tarrant J, Cain G, Lewin-Koh SC, Dybdal N, Wong H, Blackwood E, West K, Steigerwalt R, Mamounas M, Flygare JA, Amemiya K, Dambach D, Fairbrother WJ, Diaz D. Toxicol Sci. 2013; 131:247. [PubMed: 22956632]
11. (a) Sun H, Liu L, Lu J, Bai L, Li X, Nikolovska-Coleska Z, McEachern D, Yang CY, Qiu S, Yi H, Sun D, Wang S. J Med Chem. 2011; 54:3306. [PubMed: 21462933] (b) Sun H, Liu L, Lu J, Qiu S, Yang CY, Yi H, Wang S. Bioorg Med Chem Lett. 2010; 20:3043. [PubMed: 20443226] (c) Schimmer AD, Welsh K, Pinilla C, Wang Z, Krajewska M, Bonneau MJ, Pedersen IM, Kitada S, Scott FL, Bailly-Maitre B, Glinsky G, Scudiero D, Sausville E, Salvesen G, Nefzi A, Ostresh JM, Houghten RA, Reed JC. Cancer Cell. 2004; 5:25. [PubMed: 14749124] (d) Orzaez M, Gortat A,

Sancho M, Carbajo RJ, Pineda-Lucena A, Palacios-Rodriguez Y, Perez-Paya E. Apoptosis. 2011; 16:460. [PubMed: 21340509]

12. González-Lopez M, Welsh K, Finlay D, Ardecky RJ, Ganji SR, Su Y, Yuan H, Teriete P, Mace PD, Riedl SJ, Vuori K, Reed JC, Cosford NDP. Bioorg Med Chem Lett. 2011; 21:4332–4336. [PubMed: 21680182]
13. All synthesized compounds were purified by either medium pressure silica gel chromatography or preparative HPLC using a XBridge Prep C18 column (19 × 100 mm) eluted with 0.05 % formic acid in a methanol-water gradient of 10:90 to 100:0 over 10 to 15 min. with a flow rate of 25 mL/min. Compound purity was determined using analytical HPLC/MS and NMR (^{1}H and ^{13}C). The yields for the first two steps ranged from 70 – 90% while the yields for the last step ranged from 50 – 90%. The purity of each final product was greater than 95% as determined by HPLC/MS analysis.
14. Fluorescence polarization assays were run in 20 μL volume in 384 well format with black plates. The assay solution was 25 mM Hepes at pH 7.5/1 mM tris(2-carboxyethyl)phosphine/0.005% Tween 20 and 20 nM AVPIAQK-rhodamine. XIAP BIR2 was present at 1 μM or XIAP BIR3 at 0.2 μM. Compound was present within a range of 100 μM to 6.1 nM using two fold dilutions starting at 100 μM generating a 16 point curve. Plates were read on an Analyst HT in fluorescence polarization mode with excitation at 530 nm, emission at 580 nm and a dichroic mirror at 565 nm. Resulting data in mP was fit in GraphPad Prism 5 with a non-linear regression using a sigmodial curve with variable slope.
15. Nikolovska-Coleska Z, Wang R, Fang X, Pan H, Tomita Y, Li P, Roller PP, Krajewski K, Saito N, Stuckey J, Wang S. Anal Biochem. 2004332:261. [PubMed: 15325294]
16. Spectroscopic data for compound **8q**: ^{1}H NMR (400 MHz, DMSO-d_6) δ 9.99 (1H, s), 8.80 (1H, b), 8.60 (1H, d, J = 8.5 Hz), 8.38 (1H, d, J = 8.5 Hz), 7.75 (1H, m), 7.59 (1H, m), 7.52 (1H, d, J = 5.9Hz), 7.51 (1H, m), 7.50 (4H, bm), 4.71 (1H, m), 4.34 (1H, m) 3.74 (1H, m), 3.64 (1H, b), 2.05 (1H, m), 1.40 (3H, d, J = 5.9 Hz), 1.35 (3H, d, J = 5.9 Hz), 0.88 (6H, m), ^{13}C NMR (100 MHz, DMSO-d_6) δ 171.8, 170.2, 168.5, 133.7, 133.3, 128.1, 127.9, 126.0, 125.8, 122.7, 121.6, 57.5, 56.0, 48.9, 30.7, 19.1, 17.9, 15.8. Exact mass for chemical formula: $C_{22}H_{30}N_4O_3$398.23 [M], HR-MS (ESI) 399.30 [M + H].
17. Speer KF, Cosimini CL, Splan KE. Biopolymers. 2012; 98:122. [PubMed: 22020922]
18. Eckelman BP, Drag M, Snipas SJ, Salvesen GS. Cell Death Differ. 2008; 15:920. [PubMed: 18239672]
19. Cell viability was assessed using the ATPlite 1step Luminescence Assay System (PerkinElmer Inc., Waltham, MA). Briefly, cells were seeded at 2000 cells/well in 38 μL medium with 5% FBS and allowed to attach overnight. Test compound (1 μL) was added to a final concentration of 5 μM and the cells were incubated at 37oC for 4 h. TRAIL (1 μL) was then added to the desired final concentration and the cells again incubated at 37oC for 20 h. The plates were removed to room temperature for 30 min. before addition of one half volume (20 μL) of ATPlite reagent. The plates were shaken at 1,100 rpm for 2 min. to ensure proper mixing before luminescence measurement on a BMG POLARstar Omega plate reader. PPC-1 cells were maintained in RPMI 1640 (Cellgro, Manassas, VA) with 10% (v/v) FBS (HyClone, Logan, UT), and penicillin/streptomycin/L-Glutamine (Life Technologies, Carlsbad, CA).
20. Lopez, M.; Welsh, K.; Yuan, H.; Stonich, D.; Su, Y.; Garcia, X.; Cuddy, M.; Houghten, R.; Sergienko, E.; Reed, JC.; Ardecky, R.; Reddy, S.; Finlay, D.; Vuori, K.; Dad, S.; Chung, TDY.; Cosford, NDP. Antagonists of IAP-family anti-apoptotic proteins – Probe 2 Probe Reports from the NIH Molecular Libraries Program [Internet]. Bethesda (MD): National Center for Biotechnology Information (US); 2010–2009.
21. Vamos, M.; Welsh, K.; Finlay, D.; San Lee, P.; Mace, PD.; Snipas, SJ.; Gonzalez, ML.; Reddy Ganji, S.; Ardecky, RJ.; Riedl, SJ.; Salvesen, GS.; Vuori, K.; Reed, JC.; Cosford, NDP. ACS Chem Biol. 2013. in press. http://pubs.acs.org/doi/abs/10.1021/cb3005512

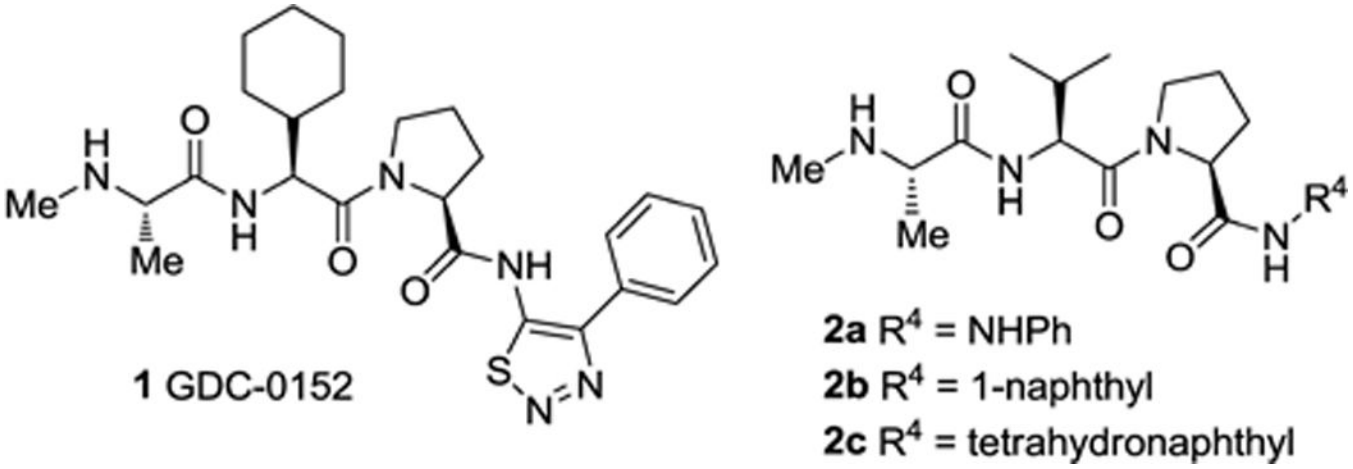

Figure 1.
Tripeptide IAP antagonists.

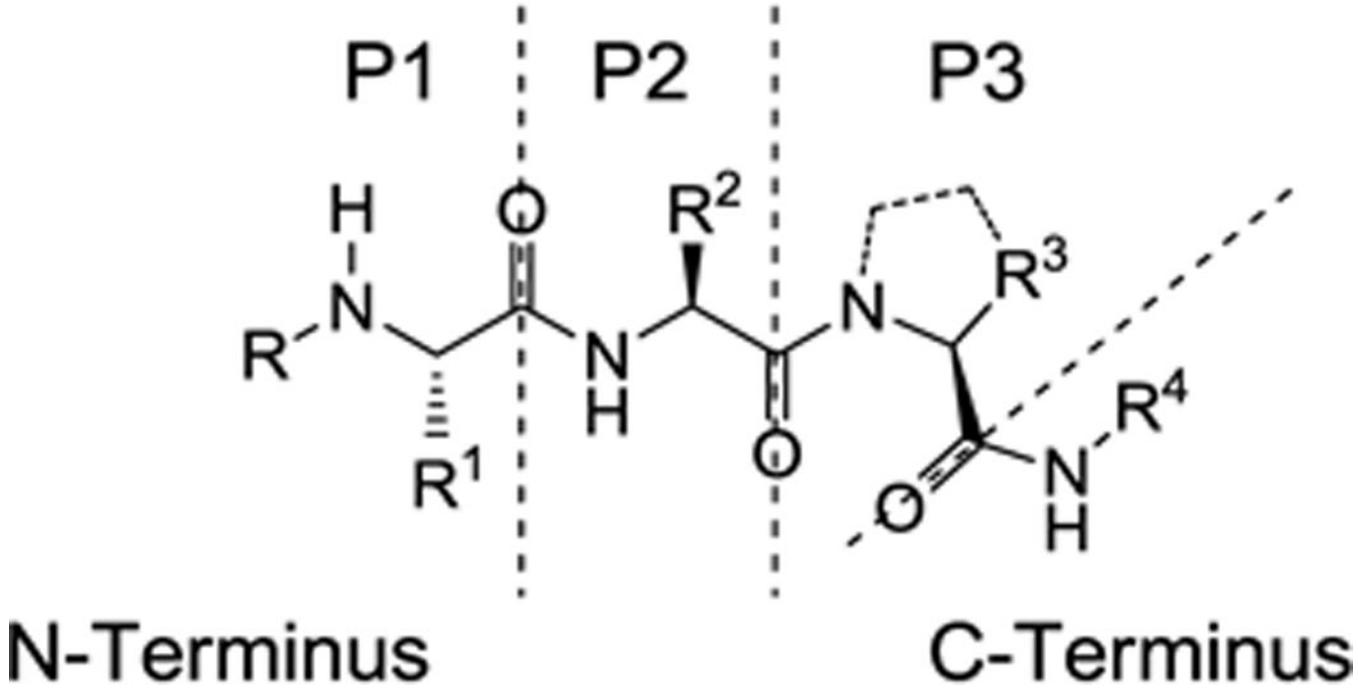

Figure 2.
Tripeptide binding model.

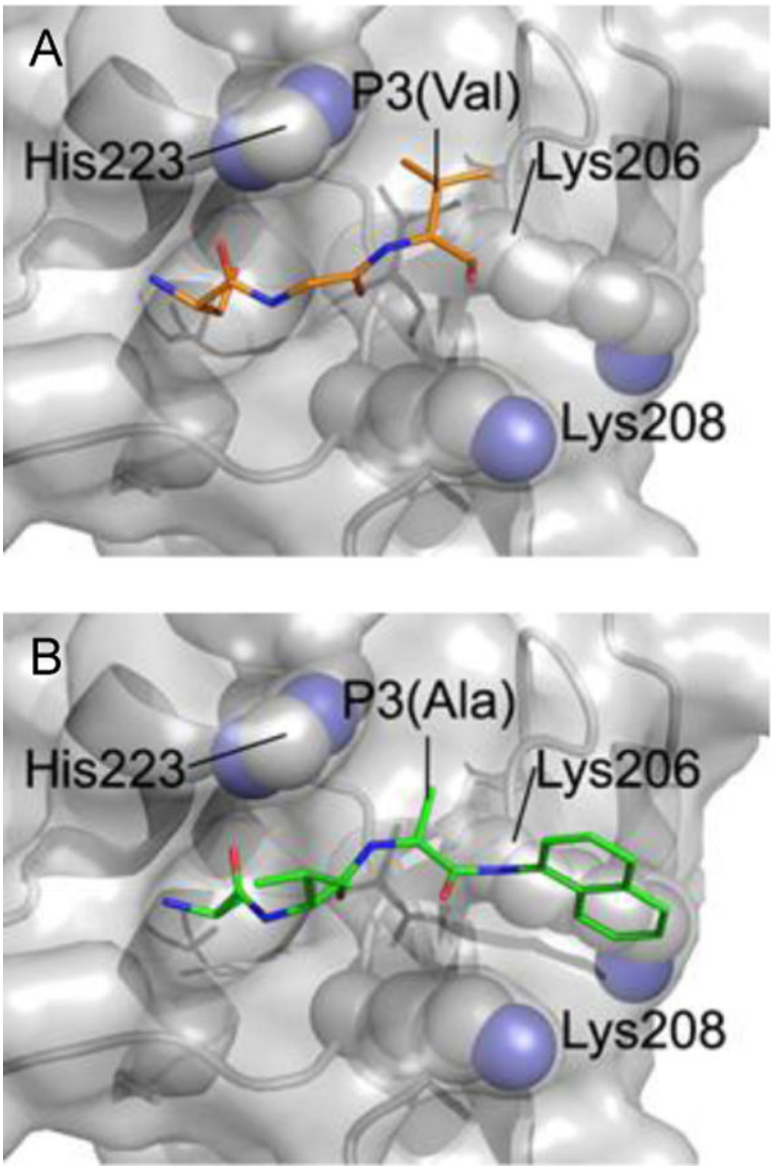

Figure 3.

Model of compound **8q** binding to XIAP BIR2. (A) Smac-like binding to BIR2 of XIAP (according to PMID 11257232; PDB 1i3o). Residues 310–312 from a neighboring Caspase-3 molecule are presented in stick form (orange) binding to the Smac-binding groove of BIR2. (B) An equivalent view of the model of **8q** (green) bound to XIAP BIR2. Residues that potentially contribute to the selectivity of **8q** are represented as spheres (C = grey, N = blue).

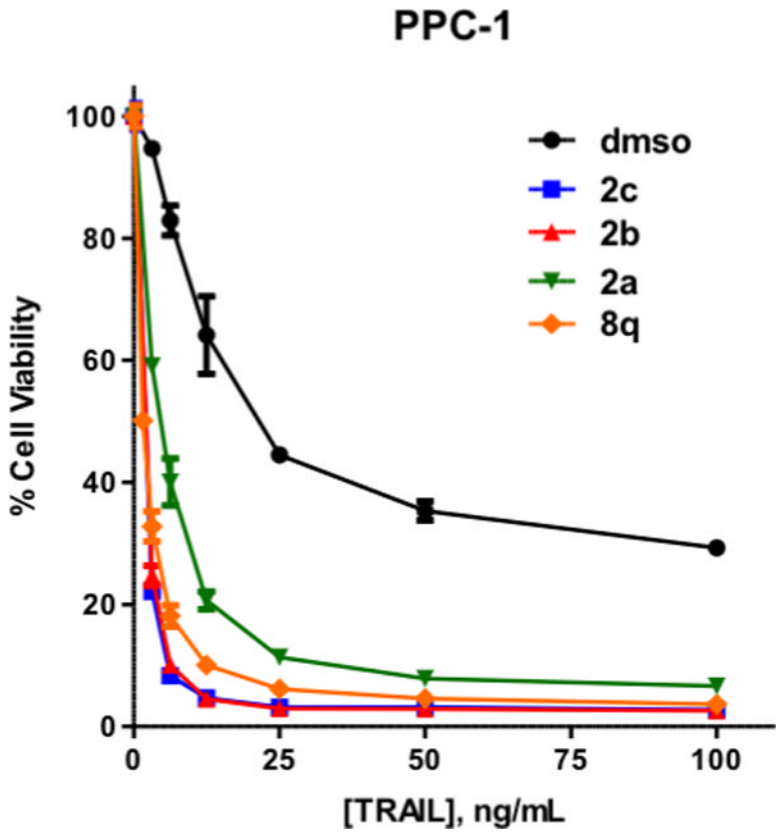

Figure 4.
TRAIL-resistant PPC-1 cells challenged with TRAIL, or compounds **2a–c** or **8q** (5 μM) alone or in the presence of TRAIL.

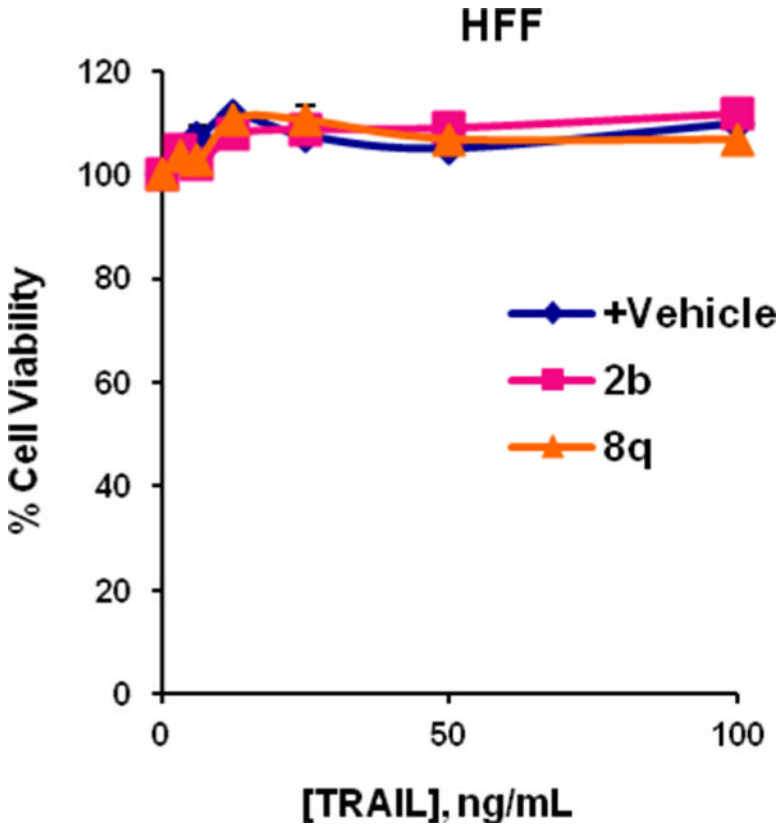

Figure 5.
Normal human foreskin fibroblasts (HFF) challenged with TRAIL, or compounds **2b** or **8q** (5 μM) alone or in the presence of TRAIL.

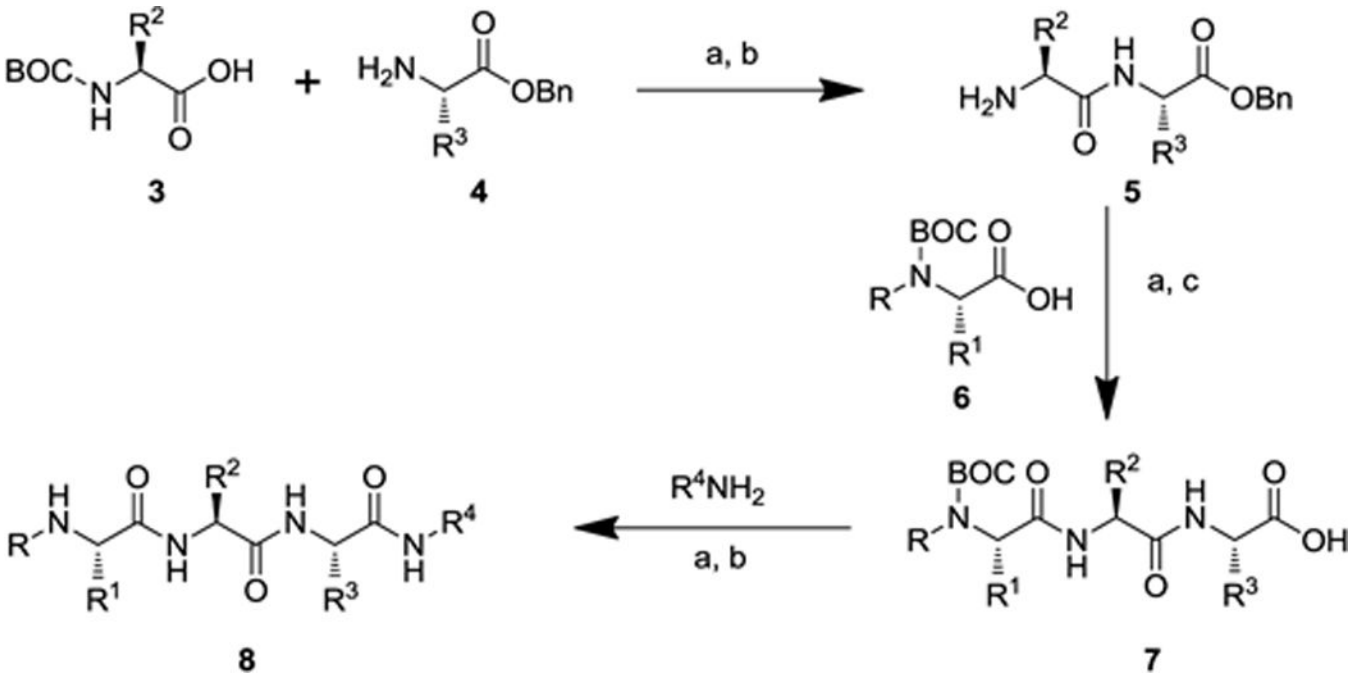

Scheme 1.

General synthetic sequence for the synthesis of small molecule IAP antagonists. Reagents and conditions: (a) EDC, HOBt, N-methylmorpholine, DMF; (b) TFA, CH_2Cl_2; (c) H_2, Pd/C, MeOH.

Table 1

Binding affinities to BIR2 or BIR3 domains of XIAP for compound **1**, and for analogues where R^4 = 1,2,3,4-tetrahydronaphthyl (**2c**, **8a–g**).

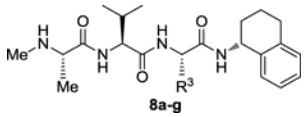

Cmpds.	P3	BIR2 K_i, μM[a]	BIR3 K_i, μM[a]	BIR2 *vs* BIR3 Selectivity
1	—	29.80 (± 4.60)	0.26 (± 0.015)	1 : 115
2c	Pro	1.37 (± 0.11)	0.06 (± 0.011)	1 : 25
8a	Ala	2.65 (± 0.15)	0.78 (± 0.11)	1 : 3.4
8b	$ArgNO_2$	3.51 (± 0.40)	0.29 (± 0.03)	1 : 12
8c	Gln	10.77 (± 1.70)	2.02 (± 0.01)	1 : 5.3
8d	LysCBZ	4.30 (± 0.18)	0.67 (± 0.04)	1 : 6.4
8e	Orn	4.36 (± 0.18)	1.13 (± 0.06)	1 : 3.9
8f	Ser	4.57 (± 0.38)	2.05 (± 0.11)	1 : 2.2
8g	OrnCBZ	2.75 (± 0.07)	0.53 (± 0.01)	1 : 5.2

[a]Values are determined in duplicate and reported ± standard deviation which is given in parentheses.

Table 2

Binding affinities to BIR2 or BIR3 domains of XIAP for tripeptide analogues where R^4 = NHPh (**2a**, **8h–p**).

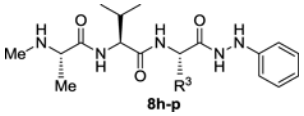

8h-p

Cmpds.	P3	BIR2 K_i, μM[a]	BIR3 K_i, μM[a]	BIR2 *vs* BIR3 Selectivity
2a	Pro	0.39 (± 0.17)	1.08 (± 0.06)	3 : 1
8h	Ala	2.29 (± 0.37)	51.79 (± 2.16)	22.6 : 1
8i	Val	3.04 (± 0.28)	65.62 (± 6.22)	21.6 : 1
8j	$ArgNO_2$	1.18 (± 0.11)	8.79 (± 1.11)	7.5 : 1
8k	Arg	3.65 (± 0.23)	21.15 (± 1.77)	5.8 : 1
8l	Thr	4.67 (± 0.37)	30.07 (± 0.55)	6.4 : 1
8m	OrnCBZ	1 70 (± 01 3)	9.82 (± 1.17)	5.8 : 1
8n	Orn	13.14 (± 1.19)	~39	3 : 1
8o	Ser	5.46 (± 0.56)	> 39	> 7.1 : 1
8p	Lys	1.88 (± 0.13)	21.48 (± 1.52)	11.4 : 1

[a]Values are determined in duplicate and reported ± standard deviation which is given in parentheses.

Table 3

Binding affinities to BIR2 or BIR3 domains of XIAP for tripeptide analogues **2b** and **8q–8y**.

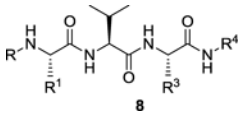

8

Cmpds.	R	R^1	P3	R^4	BIR2 K_i, µM[a]	BIR3 K_i, µM[a]	BIR2 *vs* BIR3 Selectivity
2b	CH_3	CH_3	Pro	1-naphthyl	0.44 (± 0.02)	1.51 (± 0.13)	3.4 : 1
8q	CH_3	CH_3	Ala	1-naphthyl	1.74 (± 0.30)	> 39	> 22.4 : 1
8r	CH_3	CH_3	Val	1-naphthyl	4.54 (± 0.23)	> 39	> 8.6 : 1
8s	CH_3	CH_3	OrnCBZ	1-naphthyl	1.94 (± 0.11)	> 39	> 20.1 : 1
8t	H	CH_3	Ala	1-naphthyl	0.64 (± 0.01)	40.15 (± 2.69)	62.7 : 1
8u	H	CH_2OH	Ala	1-naphthyl	2.43 (± 0.25)	> 39	> 16 : 1
8v	H	CH_2CH_3	Ala	1-naphthyl	3.78 (± 0.37)	> 39	> 10.3 : 1
8w	CH_3	CH_3	Ala	CH_2-1-naphthyl	3.00 (± 0.40)	34.18 (± 2.15)	11.4 : 1
8x	H	CH_3	Ala	NHPh	1.83 (± 0.19)	41.32 (± 0.86)	22.6 : 1
8y	CH_3	CH_3	Val	NH-3-FPh	2.38 (± 0.28)	> 39	> 16.4 : 1

[a]Values are determined in duplicate and reported ± standard deviation which is given in parentheses.